

Enlarged Kuramoto Model: Secondary Instability and Transition to Collective Chaos

Iván León and Diego Pazó

Instituto de Física de Cantabria (IFCA), Universidad de Cantabria-CSIC, 39005 Santander, Spain

(Dated: April 19, 2022)

The emergence of collective synchrony from an incoherent state is a phenomenon essentially described by the Kuramoto model. This canonical model was derived perturbatively, by applying phase reduction to an ensemble of heterogeneous, globally coupled Stuart-Landau oscillators. This derivation neglects nonlinearities in the coupling constant. We show here that a comprehensive analysis requires extending the Kuramoto model up to quadratic order. This ‘enlarged Kuramoto model’ comprises three-body (nonpairwise) interactions, which induce strikingly complex phenomenology at certain parameter values. As the coupling is increased, a secondary instability renders the synchronized state unstable, and subsequent bifurcations lead to collective chaos. An efficient numerical study of the thermodynamic limit, valid for Gaussian heterogeneity, is carried out by means of a Fourier-Hermite decomposition of the oscillator density.

Collective synchronization is a phenomenon in which an ensemble of heterogeneous, self-sustained oscillatory units (commonly known as oscillators) spontaneously entrain their rhythms. This is a pervasive phenomenon observed in natural systems and man-made devices, covering a wide range of spatio-temporal scales, from cell aggregates to swarms of fireflies [1, 2].

Seeking to understand the onset of collective synchronization, Winfree invented a model consisting of globally coupled oscillatory units with one degree of freedom (phase oscillators) [3, 4]. Following this scheme, Kuramoto found an analytically tractable model, which captures the onset of collective synchronization from an incoherent state [5, 6]. Due to its simplicity, the Kuramoto model and its generalization with phase-lagged coupling—the so-called Kuramoto-Sakaguchi model after Ref. [7]—, have been intensely studied, with a vast number of extensions and applications in several fields [8, 9].

The Kuramoto(-Sakaguchi) model is often introduced as above, i.e. as a mere mathematical refinement of the Winfree model. However, this is only partly true, since Kuramoto rigorously derived the model bearing his name. In particular, he applied phase reduction to an ensemble of weakly coupled Stuart-Landau oscillators [5, 6]. The Stuart-Landau oscillator is a relevant natural choice, as it represents a generic limit-cycle attractor close to a Hopf bifurcation.

Kuramoto’s perturbative phase-reduction approach is valid for weak coupling. Specifically, oscillator heterogeneity and interactions appear at zeroth and linear orders in the coupling constant, respectively. These considerations explain why the quadratic order was neglected in the original Kuramoto model. Nevertheless, in certain circumstances, going beyond the first (or linear) order may be required. Indeed, the description of some experiments with lattices of optomechanical [10] and nanoelectromechanical [11] oscillators rely on second-order phase reductions. The analysis of the corresponding second-order phase-reduced models has remained, however, rather incomplete. The reason for this is the nonpairwise interactions appearing at quadratic order. From this perspective, the original setup with heterogeneous, diffusively coupled Stuart-Landau oscillators appears to be the

ideal testbed model for investigating second-order phase reduction to the fullest extent possible. So far, only the case of identical oscillators has been analyzed [12].

Recently, nonpairwise (also called ‘higher-order’) interactions are attracting growing attention in several fields, such as neuroscience, ecology, and social systems (see Refs. [13, 14] and references therein). In this spirit, several works have considered populations of phase oscillators with nonpairwise interactions from the outset. Simplifying ad-hoc assumptions, such as absent pairwise coupling [15–18] and/or particularly convenient nonpairwise interactions [18–21] (e.g. admitting the Ott-Antonsen ansatz [22]), are adopted seeking analytical tractability.

In this Letter we extend the Kuramoto model up to second order in the coupling constant ϵ . In this “enlarged” Kuramoto model the new terms of order ϵ^2 comprise two different three-body (nonpairwise) interactions. Strikingly, their combined action triggers a secondary instability in which standard collective synchronization destabilizes. This is the precursor of a sequence of instabilities giving rise to a state of collective chaos. We efficiently investigate the thermodynamic limit of the model by means of a Fourier-Hermite decomposition of the oscillator density. This scheme appeared some years ago in a theoretical study [23], but it is numerically implemented here for the first time (adopting an appropriate closure).

The starting point of our work is a heterogeneous population of $N \gg 1$ Stuart-Landau oscillators with global diffusive coupling:

$$\dot{A}_j = (1 + i\sigma\omega_j)A_j - (1 + ic_2)|A_j|^2 A_j + \epsilon(1 + ic_1)(\bar{A} - A_j). \quad (1)$$

Here $A_j \equiv r_j e^{i\phi_j}$ is a complex variable, and index j runs from 1 to N . The ω_j ’s are drawn from a unit-variance normal distribution $g(\omega)$. The mean of $g(\omega)$ is selected to be 0, by going to a rotating frame if necessary. Therefore, each individual Stuart-Landau oscillator possesses a natural frequency equal to $\sigma\omega_j - c_2$, where c_2 is the nonisochronicity parameter. Parameter $\sigma > 0$ is included to account for the frequency dispersion. Concerning the coupling, it is diffusive through the mean field $\bar{A} = \frac{1}{N} \sum_{i=1}^N A_i$. Parameter $\epsilon > 0$ controls the coupling strength, and c_1 modulates its reactivity. We are exclusively interested in the thermodynamic limit ($N \rightarrow \infty$)

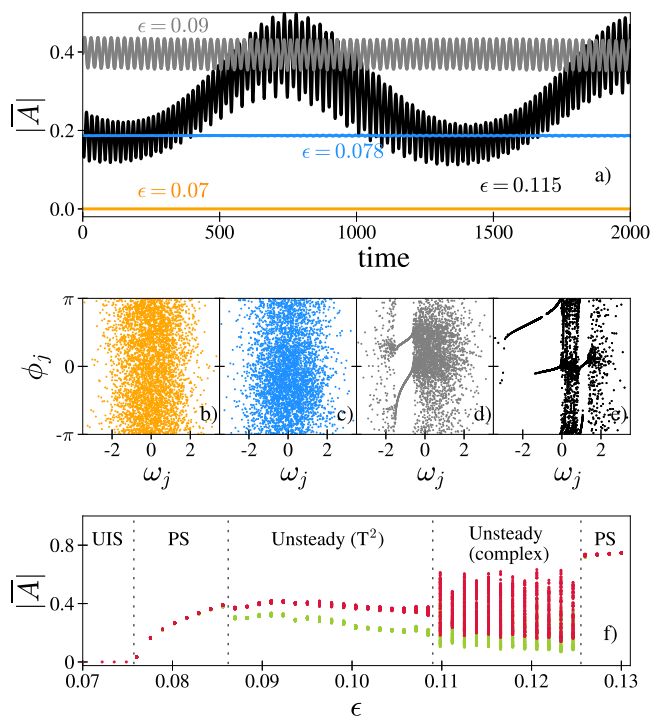


FIG. 1. Dynamics of the population of 20000 Stuart-Landau oscillators, Eq. (1), for different values of ϵ with $c_1 = -0.4$, $c_2 = 3$, and $\sigma = 10^{-3}$. (a) Time series of the mean field amplitude $|\bar{A}|$ for $\epsilon = 0.07, 0.078, 0.09$, and 0.115 . $|\bar{A}| \simeq 0$, $|\bar{A}| \simeq \text{const.} > 0$, and periodic $|\bar{A}(t)|$ correspond to UIS, PS, and quasiperiodic global attractor, respectively. (b,c,d,e) Snapshots of the angular variables ϕ_j for each of the four ϵ values chosen in (a). Only a subset of 4000 oscillators are shown for clarity. (f) Local maxima and minima of $|\bar{A}|$ as constant ϵ is increased by steps of size 1.35×10^{-3} .

of the model. In this work we select $\sigma = 10^{-3}$ and $c_2 = 3$ (a standard value in the literature, see e.g. [24]), leaving c_1 and ϵ as control parameters. The effect of varying c_2 and σ is discussed at the end of this Letter.

System (1) displays a plethora of complex states. In particular, collective chaos already emerges at moderate and large coupling under simplifying assumptions such as, homogeneity ($\sigma = 0$) [24, 25] and vanishing reactivity and shear ($c_1 = c_2 = 0$) [26]. We focus here on the weak coupling regime, in which the oscillators remain close to their original limit cycles at $r_j = 1$ and a phase description becomes possible. Two states are generically expected for small ϵ . On the one hand, there is the uniform incoherent state (UIS), corresponding to a vanishing mean field \bar{A} (in the thermodynamic limit), with the oscillators angles ϕ_j uniformly scattered, see Figs. 1(a) and 1(b) for particular parameter values and $\epsilon = 0.07$. On the other hand, typically, as ϵ exceeds a certain threshold UIS becomes unstable and a state of collective partial synchrony (PS) emerges. In this configuration, a

macroscopic proportion of the oscillators becomes entrained to a common frequency $\langle \dot{\phi}_{j \in S} \rangle = \Omega$ and the mean field rotates uniformly with constant amplitude: $|\bar{A}| = \text{const.}$ In a finite population, as in Fig. 1(c), entrained oscillators may not be observed, since they belong to one of the tails of $g(\omega)$. Drifting oscillators alone cause \bar{A} to depart from zero. Surprisingly, our numerical simulations indicate that the dynamics may become of a different kind as the coupling is further increased, while still remaining small. As shown in Fig. 1(a) for $\epsilon = 0.09$, the collective dynamics incorporates a new frequency, and $|\bar{A}(t)|$ oscillates periodically, i.e. the attractor is a two-dimensional torus or T^2 (disregarding finite-size fluctuations). Figure 1(d) shows the corresponding snapshot of the angles ϕ_j for $\epsilon = 0.09$. We may see that part of the population forms a two-cluster state that evolves in time such that the phase differences are time-dependent but bounded. As far as we know, this unsteady configuration with time-dependent clusters has not been observed before in Eq. (1). It is very much alike the Bellerophon state coined in [27] for ensembles of phase oscillators. For still larger ϵ , $|\bar{A}|$ exhibits even more complex oscillations, as can be seen setting $\epsilon = 0.115$ in Fig. 1(a). In Fig. 1(f) we represent the local maxima and minima of $|\bar{A}(t)|$ as a function of ϵ . The low-frequency modulation sets in at $\epsilon \approx 0.109$. As a result of the instability, a three-frequency quasiperiodic collective motion is, in principle, expected. Still, an additional transition to weak collective chaos cannot be ruled out. At some parameter values (e.g. $\epsilon = 0.14$, $c_1 = -0.415$), see the Supplemental Material, the largest Lyapunov exponent does not decay to zero with the system size, what is a clear indication of collective chaos. (For the value $\epsilon = 0.115$ taken in Fig. 1 the result is inconclusive.)

To put the previous observations in a wider framework we numerically determined where the unsteady behavior occurs in the $c_1 - \epsilon$ plane. The phase diagram in Fig. 2(a) shows where qualitatively different dynamics are observed. The stability boundary of UIS was analytically computed following the approach in [28], see the Supplemental Material. Remarkably, numerical simulations of Eq. (1) reveal that PS is unstable inside the dark shaded region in Fig. 2(a), i.e. unsteady $|\bar{A}(t)|$ spontaneously sets in. In addition, numerical continuation discloses an adjacent narrow band of coexistence between unsteady dynamics and PS. The orange line in Fig. 2(a) divides the unsteady region into two parts: the lower one with T^2 collective motion, and the upper one with more complex oscillations. We emphasize that determining the exact nature of the complex unsteady states is an arduous work, which hinders a more detailed phase diagram.

At this point, we resort to phase reduction in order to better understand the nature and organization of the unsteady collective states. For weak coupling phase reduction allows us to describe the system solely in terms of phase variables $\theta_j = \phi_j - c_2 \ln r_j$ [2, 6]. Following [12] we write down the second-order phase reduction [29] of (1), or ‘enlarged Kuramoto model’:

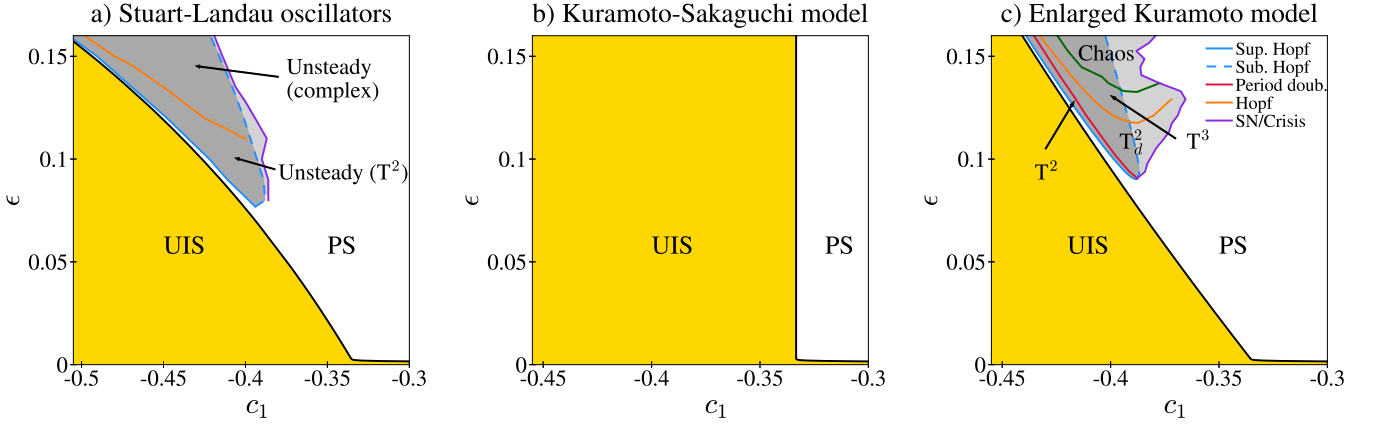


FIG. 2. Phase diagrams of model (1) for $c_2 = 3$ and $\sigma = 10^{-3}$, as well as its first- and second-order phase reductions. (a) Model (1): all boundaries were obtained from numerical simulations with a population of $N = 20000$ Stuart-Landau oscillators, save the boundary of UIS (obtained analytically). In the dark shaded region UIS and PS are both unstable, and $|\bar{A}|$ varies with time. In the light shaded region PS coexists with an unsteady state. (b) Kuramoto-Sakaguchi model obtained from Eq. (2) discarding quadratic terms in ϵ . (c) Enlarged Kuramoto model, Eq. (2); all boundaries, except the UIS-PS line, were determined using Eq. (5). The right boundary of the bistability region (in purple color) indicates where the attractor with unsteady dynamics abruptly disappears, indistinctively through a saddle-node bifurcation of tori, a boundary crisis, or any other bifurcation.

$$\dot{\theta}_j = \sigma\omega_j + \epsilon\eta R \sin(\Psi - \theta_j + \alpha) + \frac{\epsilon^2\eta^2}{4} [R \sin(\Psi - \theta_j + \beta) - R^2 \sin(2\Psi - 2\theta_j + \beta) + RQ \sin(\Phi - \Psi - \theta_j)], \quad (2)$$

where three new constants, depending on c_1 and c_2 , are defined: $\eta \equiv \sqrt{(1+c_2^2)(1+c_1^2)}$; and the phase lags $\alpha \equiv \arg[1 + c_1c_2 + (c_1 - c_2)i]$, and $\beta \equiv \arg(1 - c_1^2 + 2c_1i)$. For simplicity, we have chosen a reference frame with vanishing central frequency. Interactions involve two mean fields, $Z_1 \equiv R e^{i\Psi}$ and $Z_2 \equiv Q e^{i\Phi}$, which are the first two elements of an infinite set of Kuramoto-Daido order parameters [30]: $Z_k \equiv N^{-1} \sum_{j=1}^N e^{ik\theta_j}$. Equation (2) includes nonpairwise interactions, which are inherent to higher-order phase reduction, even if the coupling in the original system (1) is pairwise and linear [12, 31, 32]. In particular, three-body interactions are conveyed by the last two terms [33] and are comparatively weak (of order ϵ^2), as usual in physics [34]. This is not the case of most previous studies on coupled phase oscillators [15–17, 19, 20, 35, 36], but see [11, 12, 32, 37].

We start the analysis of Eq. (2) noticing that if we neglect the $O(\epsilon^2)$ terms, then we recover the Kuramoto-Sakaguchi model with coupling constant $\epsilon\eta$. For $N \rightarrow \infty$, the phase diagram resulting from this $O(\epsilon)$ approximation is shown in Fig. 2(b). The only attracting configurations are UIS and PS. The boundary of UIS can be calculated following [7]. It diverges at $c_1 = -c_2^{-1} = -1/3$, corresponding to $\alpha = -\pi/2$. When comparing Figs. 2(a) and 2(b), it is manifest that first-order phase reduction does not provide a faithful description of system (1) in the left part of the phase diagram.

We now consider Eq. (2) in full. Concerning the linear stability of UIS ($R = Q = 0$), only the first term of order ϵ^2 is relevant. It may be added to the linear term to recalculate the stability boundary [7], see the Supplemental Material. The

result is shown as a solid black line in Fig. 2(c). Now the boundary of UIS exhibits a knee at $c_1 \approx -1/3$, in qualitative agreement with Fig. 2(a). Analyzing the stability of PS is a much harder problem. Through a numerical self-consistent approach [7] we tracked the branch of PS emanating from incoherence. However, this does not allow us to determine its stability. Moreover, the direct numerical integration of Eq. (2) is not more efficient than simulating Eq. (1): The number of degrees of freedom is reduced by a factor 2, but at the cost of including computationally expensive trigonometric functions.

In order to exploit the dimensionality reduction achieved in Eq. (2), an alternative strategy is required. We resort to a moments system introduced almost a decade ago by Chiba in his theoretical study of the Kuramoto model [23]. Crucially, working with a set of moments avoids finite-size fluctuations and the concomitant microscopic (phase) chaos [38]. We start defining the density $\rho(\theta|\omega, t)$, such that $\rho(\theta|\omega, t)d\theta$ is the fraction of oscillators with phases between θ and $\theta + d\theta$ and frequency ω at time t . Now, we write the Fourier-Hermite decomposition of ρ :

$$\rho(\theta|\omega, t) = \frac{1}{2\pi} \sum_{k=-\infty}^{\infty} \sum_{m=0}^{\infty} P_k^m(t) e^{-ik\theta} h_m(\omega), \quad (3)$$

where $h_m(x) = \text{He}_m(x)/\sqrt{m!}$ are normalized (probabilist's) Hermite polynomials: $\int_{-\infty}^{\infty} h_m(\omega) h_n(\omega) g(\omega) d\omega = \delta_{mn}$. The Fourier-Hermite coefficients P_k^m are obtained inverting

Eq. (3):

$$P_k^m(t) = \int_0^{2\pi} d\theta e^{ik\theta} \int_{-\infty}^{\infty} d\omega h_m(\omega) g(\omega) \rho(\theta|\omega, t). \quad (4)$$

These Fourier-Hermite modes extend the Kuramoto-Daido order parameters to the space of the natural frequencies. Specifically, $P_k^0 = Z_k$ (in the $N \rightarrow \infty$ limit). The density ρ obeys the continuity equation $\partial_t \rho = -\partial_\theta(\rho \dot{\theta})$. Inserting the expansion (3), using the recurrence relation $\omega h_m = \sqrt{m} h_{m-1} + \sqrt{m+1} h_{m+1}$ [39], and redefining $P_k^m \rightarrow (-i)^m P_k^m$ for convenience, we get an infinite set of ordinary differential equations:

$$\begin{aligned} k^{-1} \dot{P}_k^m &= \sigma (\sqrt{m} P_k^{m-1} - \sqrt{m+1} P_k^{m+1}) \\ &+ \frac{\epsilon \eta}{2} (P_{k-1}^m Z_1 e^{i\alpha} - P_{k+1}^m Z_1^* e^{-i\alpha}) \\ &+ \frac{\epsilon^2 \eta^2}{8} (P_{k-1}^m Z_1 e^{i\beta} - P_{k+1}^m Z_1^* e^{-i\beta} - P_{k-2}^m Z_1^2 e^{i\beta} \\ &+ P_{k+2}^m Z_1^{*2} e^{-i\beta} + P_{k-1}^m Z_2 Z_1^* - P_{k+1}^m Z_2^* Z_1), \quad (5) \end{aligned}$$

where the asterisk denotes complex conjugation. System (5) is equivalent to Eq. (2) with $N \rightarrow \infty$.

The numerical integration of Eq. (5) requires to implement a truncation at finite k_{\max} and m_{\max} , with an adequate closure. Note first that, in the UIS, $P_0^0 = 1$ is the only nonzero coefficient, whereas in the PS state the modes decay with k and m roughly as $|P_k^m| \sim e^{-ak} e^{-b\sqrt{m}}$. We imposed the boundary conditions: $P_{k_{\max}+1}^m = 0$, and $P_k^{m_{\max}+1} = 2P_k^{m_{\max}} - P_k^{m_{\max}-1}$. We tested the performance of different system sizes, finding that $k_{\max} = m_{\max} = 40$ already yield an excellent convergence, even for strongly unsteady states. Therefore, our analysis below relies on Eq. (5) with $n_f = k_{\max} \times (m_{\max} + 1) \times 2 = 3280$ degrees of freedom. In comparison, simulating Eq. (2) with n_f oscillators is unproductive because of unavoidable finite-size fluctuations.

One now can see that the PS state corresponds to a solid rotation $P_k^m(t) = p_k^m e^{ik\Omega t}$. After inserting this solution into Eq. (5), the unknowns p_k^m and Ω are found via a Newton-Raphson algorithm (imposing $p_1^1 \in \mathbb{R}$). The result completely agrees with the one obtained from the self-consistent numerical calculation mentioned above. Now, however, we can determine linear stability. Moving to a rotating frame with angular velocity Ω , we linearize the system around the fixed point. The locus of a secondary (Hopf) instability is accurately located requiring the eigenvalues of the Jacobian matrix with the largest real part to be $\pm i\Omega_H$ (with an extra zero eigenvalue due to rotational invariance $P_k^m \rightarrow e^{ik\gamma} P_k^m$). The Hopf line is shown in blue in Fig. 2(c). The transition is supercritical (subcritical) at the solid (dashed) line. The emerging oscillatory mode yields a torus attractor (T^2), in which, due to the rotational symmetry, no lockings on its surface are expected, see e.g. [40, 41]. Recalling Eq. (2) we infer that, at the level of the individual oscillators, the superimposed oscillation induces entrainment at frequencies $\Omega + (n/2)\Omega_H$ ($n \in \mathbb{Z}$). The half-integer frequency plateaus stem from the term accompanying R^2 in Eq. (2). In particular, the two clusters in Fig. 1(d) correspond to a frequency plateau at frequency $\Omega + \Omega_H/2$.

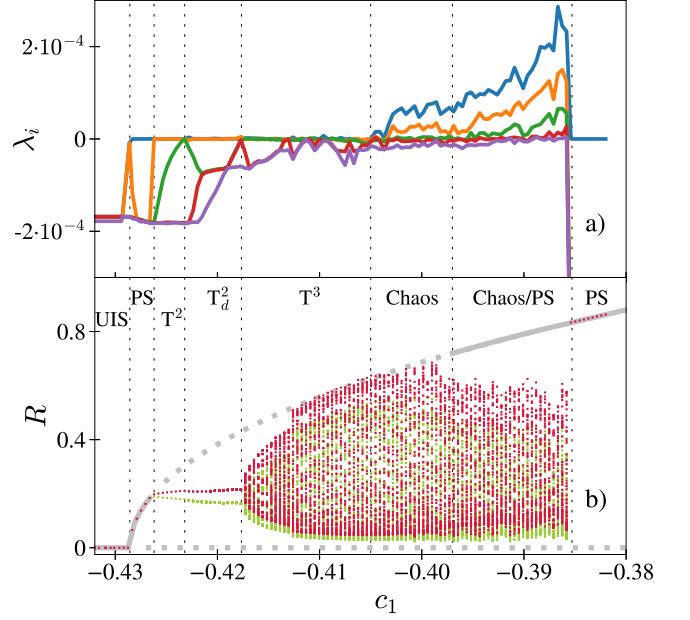


FIG. 3. Sequence of bifurcations of Eq. (2), obtained from Eq. (5), as c_1 is increased with $\epsilon = 0.14$. (a) Five largest Lyapunov exponents $\{\lambda_i\}_{i=1,\dots,5}$. (b) Local maxima and minima of $R(t)$. As a reference, the R values of UIS ($R = 0$) and PS ($R > 0$) are depicted in gray. Solid (dashed) lines correspond to linearly stable (unstable) states.

The remaining regions of the phase diagram in Fig. 2(c) are determined from direct numerical simulations of Eq. (5) with the aforementioned closure, as well as by computing the largest Lyapunov exponents $\{\lambda_i\}_{i=1,2,\dots}$. Our systematic exploration reveals a period-doubling bifurcation line ($T^2 \rightarrow T_d^2$ transition) close to the supercritical-Hopf line. The period-doubling bifurcation line almost certainly exists also for the ensemble of Stuart-Landau oscillators. Magnifying the gray line in Fig. 1(a) the signature of a doubled torus T_d^2 can be discerned. However, it is very hard to determine the bifurcation point due to the long transients involved and unavoidable finite-size fluctuations, see Fig. 1(f).

As occurs with the ensemble of Stuart-Landau oscillators, the torus attractor undergoes a Hopf bifurcation, see the orange line in Fig. 2(c). Thereby three-frequency quasiperiodic dynamics (T^3 attractor) emerges, consistently with three vanishing Lyapunov exponents.

Adjacent to the T^3 domain in Fig. 2(c), there exists a region with chaotic dynamics, in conformity with the Ruelle-Takens-Newhouse scenario. As occurred with system (1), Fig. 2(a), PS and unsteady states coexist. In Fig. 2(c) the bistability region is bounded by a purple line denoting either a saddle-node bifurcation, emanating from a (codimension-2) Bautin point at the bottom of the Hopf line, or an attractor crisis. The phase diagram in Fig. 2(c) reveals which are the unsteady collective states of (1), and their expected arrangement. Indeed, obtaining a phase diagram with the degree of detail of Fig. 2(c) is virtually unattainable simulating the original system, Eq. (1).

To better characterize the chaotic region, a detailed explo-

ration along the horizontal line $\epsilon = 0.14$ is shown in Fig. 3. In Figs. 3(a) and 3(b) the five largest Lyapunov exponents and the local maxima and minima of $|P_1^0(t)| = R(t)$ are, respectively, depicted for the same c_1 range. In the T^3 interval there may be some additional bifurcations (lockings or torus doubling), which we did not attempt to resolve. Interestingly, in the chaotic domain an increasing number of Lyapunov exponents become positive as c_1 increases, i.e. collective chaos transforms into collective hyperchaos.

In this Letter we have introduced the ‘enlarged Kuramoto model’; a population of phase oscillators in which three-body interactions enter in a perturbative way. Remarkably, this makes a world of difference, drastically reshaping the traditional Kuramoto scenario. The ‘enlarged Kuramoto model’ exhibits a variety of unsteady states, including collective chaos and hyperchaos. To our knowledge, these states have not been previously reported in a population of globally coupled phase oscillators, with a unimodal distribution of the natural frequencies. We have considered a particular frequency dispersion $\sigma = 10^{-3}$ in Fig. 2(c). If σ is lowered the bottom of the Hopf bifurcation line approaches the c_1 axis at $c_1 = -c_2^{-1}$. This is expected to occur for any nonzero c_2 value, in consistence with the $\sigma = 0$ case [12] (to be shown elsewhere). Nonetheless, only heterogeneity, in contradistinction to weak noise [12, 42], is able to trigger unsteady collective dynamics (absent for $\sigma = 0$). As a final remark, we stress that reducing the population of Stuart-Landau oscillators (1) to the phase model (2) is both illuminating and convenient, as it enables an efficient investigation of the thermodynamic limit by virtue of the Fourier-Hermite expansion. The application of this scheme to other populations of phase oscillators with Gaussian heterogeneity is straightforward. For other forms of $g(\omega)$ the suitable set of orthogonal polynomials must be adopted: e.g. the Fourier-Legendre mode decomposition is appropriate for uniform $g(\omega)$.

We thank Ernest Montbrí and Juan M. López for their critical reading of the manuscript. We acknowledge support by Agencia Estatal de Investigación and Fondo Europeo de Desarrollo Regional under Project No. FIS2016-74957-P (AEI/FEDER, EU). IL acknowledges support by Universidad de Cantabria and Government of Cantabria under the Concepción Arenal programme.

-
- [1] S. H. Strogatz, *Sync: The emerging science of spontaneous order* (Hyperion Press, New York, 2003).
- [2] A. S. Pikovsky, M. G. Rosenblum, and J. Kurths, *Synchronization, a Universal Concept in Nonlinear Sciences* (Cambridge University Press, Cambridge, 2001).
- [3] A. T. Winfree, “Biological rhythms and the behavior of populations of coupled oscillators.” *J. Theor. Biol.* **16**, 15–42 (1967).
- [4] A. T. Winfree, *The Geometry of Biological Time* (Springer, New York, 1980).
- [5] Y. Kuramoto, “Self-entrainment of a population of coupled nonlinear oscillators,” in *International Symposium on Mathemat-*

- cal Problems in Theoretical Physics*, Lecture Notes in Physics, Vol. 39, edited by Huzihiro Araki (Springer, Berlin, 1975) pp. 420–422.
- [6] Y. Kuramoto, *Chemical Oscillations, Waves, and Turbulence* (Springer-Verlag, Berlin, 1984).
- [7] H. Sakaguchi and Y. Kuramoto, “A soluble active rotator model showing phase transitions via mutual entrainment,” *Prog. Theor. Phys.* **76**, 576–581 (1986).
- [8] J. A. Acebrón, L. L. Bonilla, C. J. Pérez-Vicente, F. Ritort, and R. Spigler, “The Kuramoto model: A simple paradigm for synchronization phenomena,” *Rev. Mod. Phys.* **77**, 137–185 (2005).
- [9] F. A. Rodrigues, T. K. DM. Peron, P. Ji, and J. Kurths, “The Kuramoto model in complex networks,” *Physics Reports* **610**, 1–98 (2016).
- [10] Georg Heinrich, Max Ludwig, Jiang Qian, Björn Kubala, and Florian Marquardt, “Collective dynamics in optomechanical arrays,” *Phys. Rev. Lett.* **107**, 043603 (2011).
- [11] M. H. Matheny, J. Emenheiser, W. Fon, A. Chapman, A. Salova, M. Rohden, J. Li, M. Hudoba de Badyn, M. Pósfai, L. Duenas-Osorio, M. Mesbahi, J. P. Crutchfield, M. C. Cross, R. M. D’Souza, and M. L. Roukes, “Exotic states in a simple network of nanoelectromechanical oscillators,” *Science* **363**, eaav7932 (2019).
- [12] I. León and D. Pazó, “Phase reduction beyond the first order: The case of the mean-field complex Ginzburg-Landau equation,” *Phys. Rev. E* **100**, 012211 (2019).
- [13] Tomislav Stankovski, Tiago Pereira, Peter V. E. McClintock, and Aneta Stefanovska, “Coupling functions: Universal insights into dynamical interaction mechanisms,” *Rev. Mod. Phys.* **89**, 045001 (2017).
- [14] F. Battiston, G. Cencetti, I. Iacopini, V. Latora, M. Lucas, A. Patania, J.-G. Young, and G. Petri, “Networks beyond pairwise interactions: Structure and dynamics,” *Phys. Rep.* **874**, 1–92 (2020).
- [15] T. Tanaka and T. Aoyagi, “Multistable attractors in a network of phase oscillators with three-body interactions,” *Phys. Rev. Lett.* **106**, 224101 (2011).
- [16] Maxim Komarov and Arkady Pikovsky, “Finite-size-induced transitions to synchrony in oscillator ensembles with nonlinear global coupling,” *Phys. Rev. E* **92**, 020901(R) (2015).
- [17] C. Xu and P. S. Skardal, “Spectrum of extensive multiclusters in the Kuramoto model with higher-order interactions,” *Phys. Rev. Research* **3**, 013013 (2021).
- [18] Xuan Wang, Zhigang Zheng, and Can Xu, “Collective dynamics of phase oscillator populations with three-body interactions,” *Phys. Rev. E* **104**, 054208 (2021).
- [19] Per Sebastian Skardal and Alex Arenas, “Abrupt desynchronization and extensive multistability in globally coupled oscillator simplexes,” *Phys. Rev. Lett.* **122**, 248301 (2019).
- [20] Per Sebastian Skardal and Alex Arenas, “Higher order interactions in complex networks of phase oscillators promote abrupt synchronization switching,” *Communications Physics* **3**, 218 (2020).
- [21] M. Lucas, G. Cencetti, and F. Battiston, “Multiorder Laplacian for synchronization in higher-order networks,” *Phys. Rev. Research* **2**, 033410 (2020).
- [22] E. Ott and T. M. Antonsen, “Low dimensional behavior of large systems of globally coupled oscillators,” *Chaos* **18**, 037113 (2008).
- [23] H. Chiba, “Continuous limit and the moments system for the globally coupled phase oscillators,” *Discrete and Continuous Dynamical Systems-Series A* **33**, 1891–1903 (2013).
- [24] N. Nakagawa and Y. Kuramoto, “Collective chaos in a popu-

- lation of globally coupled oscillators,” *Prog. Theor. Phys.* **89**, 313–323 (1993); P. Clusella and A. Politi, “Between phase and amplitude oscillators,” *Phys. Rev. E* **99**, 062201 (2019).
- [25] V. Hakim and W. J. Rappel, “Dynamics of the globally coupled complex Ginzburg-Landau equation,” *Phys. Rev. A* **46**, R7347–R7350 (1992).
- [26] P. C. Matthews and S. H. Strogatz, “Phase diagram for the collective behavior of limit-cycle oscillators,” *Phys. Rev. Lett.* **65**, 1701–1704 (1990); P. C. Matthews, R. E. Mirollo, and S. H. Strogatz, “Dynamics of a large system of coupled nonlinear oscillators,” *Physica D* **52**, 293–331 (1991).
- [27] Hongjie Bi, Xin Hu, S. Boccaletti, Xingang Wang, Yong Zou, Zonghua Liu, and Shuguang Guan, “Coexistence of quantized, time dependent, clusters in globally coupled oscillators,” *Phys. Rev. Lett.* **117**, 204101 (2016); Jiameng Zhang, Stefano Boccaletti, Zonghua Liu, and Shuguang Guan, “Synchronization of phase oscillators under asymmetric and bimodal distributions of natural frequencies,” *Chaos Solit. Fractals* **136**, 109777 (2020).
- [28] M. C. Cross, J. L. Rogers, Ron Lifshitz, and A. Zumdieck, “Synchronization by reactive coupling and nonlinear frequency pulling,” *Phys. Rev. E* **73**, 036205 (2006).
- [29] A complete derivation can be found in the Supplemental Material. In Eq. (2) terms of orders $O(\epsilon^3)$ and $O(\epsilon^2\sigma)$ have been neglected, since small coupling strength ($\epsilon \ll 1$) and frequency dispersion ($\sigma \ll 1$) are assumed. Moreover, note that phase reduction does not introduce terms proportional to $\epsilon\sigma$, as in [32].
- [30] H. Daido, “Critical conditions of macroscopic mutual entrainment in uniformly coupled limit-cycle oscillators,” *Prog. Theor. Phys.* **89**, 929–934 (1993).
- [31] Y. Kuramoto and H. Nakao, “On the concept of dynamical reduction: the case of coupled oscillators,” *Phil. Trans. R. Soc. A* **377**, 20190041 (2019).
- [32] Erik Gengel, Erik Teichmann, Michael Rosenblum, and Arkady Pikovsky, “High-order phase reduction for coupled oscillators,” *J. Phys.: Complexity* **2**, 015005 (2021).
- [33] Notice these identities: $R^2 \sin(2\Psi - 2\theta_j + \beta) = N^{-2} \sum_{k,l} \sin(\theta_k + \theta_l - 2\theta_j + \beta)$; $RQ \sin(\Phi - \Psi - \theta_j) = N^{-2} \sum_{k,l} \sin(2\theta_k - \theta_l - \theta_j)$.
- [34] Hans-Werner Hammer, Andreas Nogga, and Achim Schwenk, “Colloquium: Three-body forces: From cold atoms to nuclei,” *Rev. Mod. Phys.* **85**, 197–217 (2013).
- [35] C. Bick, P. Ashwin, and A. Rodrigues, “Chaos in generically coupled phase oscillator networks with nonpairwise interactions,” *Chaos* **26**, 094814 (2016).
- [36] Per Sebastian Skardal and Alex Arenas, “Memory selection and information switching in oscillator networks with higher-order interactions,” *J. Phys.: Complexity* **2**, 015003 (2021).
- [37] Mohit Kumar and Michael Rosenblum, “Two mechanisms of remote synchronization in a chain of stuart-landau oscillators,” *Phys. Rev. E* **104**, 054202 (2021).
- [38] O. V. Popovych, Y. L. Maistrenko, and P. A. Tass, “Phase chaos in coupled oscillators,” *Phys. Rev. E* **71**, 065201(R) (2005).
- [39] M. Abramowitz and I. A. Stegun, *Handbook of Mathematical Functions* (Dover, New York, 1972).
- [40] David Rand, “Dynamics and symmetry. predictions for modulated waves in rotating fluids,” *Archive for Rational Mechanics and Analysis* **79**, 1–37 (1982).
- [41] Dwight Barkley, “Euclidean symmetry and the dynamics of rotating spiral waves,” *Phys. Rev. Lett.* **72**, 164–167 (1994).
- [42] Iván León and Diego Pazó, “Quasi phase reduction of all-to-all strongly coupled $\lambda - \omega$ oscillators near incoherent states,” *Phys. Rev. E* **102**, 042203 (2020).

**Supplemental Material to
“Enlarged Kuramoto Model: Secondary Instability and Transition to Collective Chaos”**

Iván León and Diego Pazó
Instituto de Física de Cantabria (IFCA), Universidad de Cantabria-CSIC, 39005 Santander, Spain

CONTENTS

I. Collective chaos in Eq. (1)	1
II. Boundary of Incoherence for Eq. (1)	2
Thermodynamic limit: Perturbed Density	3
Perturbation dynamics	3
Self-consistency condition	4
Final result	4
III. Derivation of Eq. (2)	5
IV. Boundary of Incoherence for Eq. (2)	6
References	6

I. COLLECTIVE CHAOS IN EQ. (1)

The ensemble of heterogeneous Stuart-Landau oscillators (Eq. (1) in the main text) exhibits a wide variety of dynamical states. In this section we show the existence of collective chaos. Collective chaos is characterized by the existence of at least one positive Lyapunov exponent (LE) in the thermodynamic limit ($N \rightarrow \infty$).

Verifying collective chaos in Eq. (1) is a hard task due to the unavoidable presence of microscopic (phase) chaos [1]. Microscopic chaos yields $n_{mic} \gg 1$ positive LEs. Crucially, although n_{mic} is proportional to the system size N , the magnitude of the corresponding LEs decays to zero as $N \rightarrow \infty$. This means that for large enough N , the largest LE associated with collective chaos will prevail. Otherwise, if the largest LE decays to zero as N grows, then collective chaos can be ruled out.

In Fig. S1 we depict the largest LE λ versus the number of oscillators N for different parameter values. We choose $c_2 = 3$, $\sigma = 10^{-3}$, $c_1 = -0.4$, and ϵ values as in Fig. 1 of the main text. Moreover, data for $c_1 = -0.415$ and $\epsilon = 0.14$ are also depicted. In the figure it can be observed that λ rapidly decays to zero for UIS (orange), PS (blue). This decaying is consistent with the $1/N$ law reported in [1]. The exponent also decays to zero (although in a slower manner) for the parameters where the T^2 is stable (gray). The LE computed for the largest ϵ value in Fig. 1, $\epsilon = 0.115$, exhibits an even slower decay. This behavior does not confirm nor refute if (weak) collective chaos is already present. For a larger value of $\epsilon = 0.14$ ($c_1 = -0.415$), collective chaos is more evident, with $\lambda \simeq 3.5 \times 10^{-4}$. These values of λ are of the same order of magnitude than those found in the enlarged Kuramoto model with collective chaos, see Fig. 3(a).

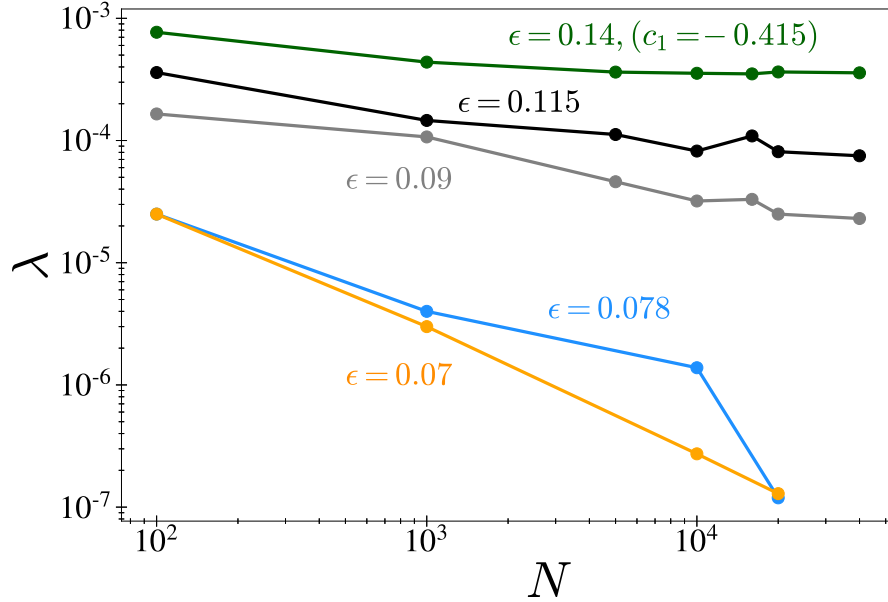


FIG. S1. Largest Lyapunov exponent for Eq. (1) in the main text as a function of the number of oscillators N . The parameter values are those used in Fig. 1 of the main text, namely $c_1 = -0.4$, $c_2 = 3$, $\sigma = 10^{-3}$ and $\epsilon = 0.07$ (orange), 0.078 (blue), 0.09 (gray), and 0.115 (black). Additionally, we selected $\epsilon = 0.14$ and $c_1 = -0.415$ (green) to show a state with clear-cut collective chaos.

II. BOUNDARY OF INCOHERENCE FOR EQ. (1)

We derive the conditions satisfied at the marginal stability of incoherence for an infinite ensemble of Stuart-Landau oscillators, Eq. (1) in the main text. This derivation follows [2].

The outline of the derivation is as follows. First we consider an infinitesimal perturbation around the uniform incoherent state (UIS), written in terms of the density of oscillators. This perturbed density evolves according to the continuity equation, but in addition it should verify the self-consistent condition. That means, the distribution has to be consistent with the mean-field it produces. At the stability boundary of incoherence the perturbation neither decays nor grows.

For simplicity, it is convenient to transform the equation of the oscillators so that in the UIS the amplitude of the oscillations is 1. This can be achieved by a change of coordinates of the oscillators $B_j = A_j \exp[i\epsilon c_1 t + i c_2(1 - \epsilon)t]/\sqrt{1 - \epsilon}$, and rescaling time $\tau = (1 - \epsilon)t$, frequency $\tilde{\omega} = \sigma\omega/(1 - \epsilon)$ and coupling

$$\kappa = \frac{\epsilon}{1 - \epsilon}. \quad (\text{S1})$$

In the new coordinates, Eq. (1) writes:

$$\frac{dB_j}{d\tau} = (1 + i\tilde{\omega}_j + i c_2)B_j - (1 + i c_2)|B_j|^2 B_j + \kappa(1 + i c_1)\bar{B}. \quad (\text{S2})$$

It is important to notice that now $\tilde{\omega}$ are distributed following a Gaussian distribution $g(\tilde{\omega})$ with standard deviation $\tilde{\sigma} = \sigma/(1 - \epsilon) = \sigma(1 + \kappa)/(1 - \kappa)$. This implies that the frequency distribution depends on κ . For convenience we write (S2) in polar coordinates:

$$\frac{dr_j}{d\tau} = \dot{r}_j = r_j - r_j^3 + \kappa|\bar{B}| [\cos(\Upsilon - \phi_j) - c_1 \sin(\Upsilon - \phi_j)], \quad (\text{S3})$$

$$\frac{d\phi_j}{d\tau} = \dot{\phi}_j = \tilde{\omega}_j + c_2(1 - r_j^2) + \frac{\kappa|\bar{B}|}{r_j} [\sin(\Upsilon - \phi_j) + c_1 \cos(\Upsilon - \phi_j)], \quad (\text{S4})$$

where the mean field is

$$\overline{B} \equiv |\overline{B}|e^{i\Upsilon}.$$

At UIS $\overline{B} = 0$ and $r_j = 1$.

Thermodynamic limit: Perturbed Density

As we are interested in the behavior in the thermodynamic limit $N \rightarrow \infty$, we can define the density distribution of oscillators $\rho(r, \phi|\tilde{\omega}, \tau)$, such that $\rho(r, \phi|\tilde{\omega}, \tau)r d\phi dr$ is the fraction of oscillators between $(r, r + dr)$ and $(\phi, \phi + d\phi)$ with frequency $\tilde{\omega}$ at time τ . In the vicinity of the UIS the density is:

$$\rho(r, \phi|\tilde{\omega}, \tau) = \frac{1}{2\pi r} \delta[r - 1 - \varepsilon r_1(\phi|\tilde{\omega}, \tau)][1 + \varepsilon f_1(\phi|\tilde{\omega}, \tau)], \quad (\text{S5})$$

where the small constant ε explicits the smallness of the deviations from the unit circle and from the uniform angular density through r_1 and f_1 , respectively. Note that the normalization condition, requires the average of f_1 over ϕ to vanish.

$$1 = \int_0^\infty r dr \int_0^{2\pi} d\phi \rho = 1 + \frac{\varepsilon}{2\pi} \int_0^{2\pi} f_1(\phi|\tilde{\omega}, \tau) d\phi.$$

Close to the UIS, the amplitude of the mean field $|\overline{B}|$ is a small quantity of order ε :

$$|\overline{B}| = \overline{B} e^{-i\Upsilon} = \int_{-\infty}^\infty d\tilde{\omega} g(\tilde{\omega}) \int_0^\infty r dr \int_0^{2\pi} d\phi \rho(r, \phi|\tilde{\omega}, \tau) r e^{i(\phi - \Upsilon)} = \frac{\varepsilon}{2\pi} \int_{-\infty}^\infty d\tilde{\omega} g(\tilde{\omega}) \int_0^{2\pi} d\phi [f_1(\phi|\tilde{\omega}, \tau) + r_1(\phi|\tilde{\omega}, \tau)] e^{i(\phi - \Upsilon)} + O(\varepsilon^2) \quad (\text{S6})$$

Perturbation dynamics

The evolution of the radial perturbation r_1 is obtained using the chain rule

$$\frac{dr}{d\tau} = \frac{\partial r}{\partial \phi} \frac{d\phi}{d\tau} + \frac{\partial r}{\partial \tau}. \quad (\text{S7})$$

Replacing (S3) and (S4) with $r = 1 + \varepsilon r_1$, $|\overline{B}| \equiv \varepsilon B_0$ and neglecting terms of order ε^2 :

$$-2r_1 + \kappa B_0 [\cos(\Upsilon - \phi) - c_1 \sin(\Upsilon - \phi)] = \frac{\partial r_1}{\partial \phi} \tilde{\omega} + \frac{\partial r_1}{\partial \tau}. \quad (\text{S8})$$

We assume an exponential growth rate λ of the perturbation. In general, λ is a pure imaginary number at threshold, however, we assume λ is real provided the frequency distribution is shifted by a certain frequency shift Ω_c , which is later obtained self-consistently. In this reference frame we can choose $\Upsilon = 0$, but we keep it for clarity. We replace $\frac{\partial r_1}{\partial \tau}$ by λr_1 in (S8). The solution has a trigonometric form:

$$r_1 = \kappa B_0 [\mathcal{A} \cos(\Upsilon - \phi) + \mathcal{B} \sin(\Upsilon - \phi)] \quad (\text{S9})$$

with

$$\mathcal{A} = \frac{2 + \lambda - c_1 \tilde{\omega}}{\tilde{\omega}^2 + (2 + \lambda)^2}, \quad \text{and} \quad \mathcal{B} = -\frac{(2 + \lambda)c_1 + \tilde{\omega}}{(2 + \lambda)^2 + \tilde{\omega}^2}.$$

Next, we calculate f_1 . First of all notice that the density ρ satisfies the continuity equation:

$$\frac{\partial \rho}{\partial \tau} + \vec{\nabla} \cdot (\rho \vec{v}) = 0, \quad (\text{S10})$$

where \vec{v} is the velocity vector. The divergence in polar coordinates is $\vec{\nabla} \cdot \vec{F} = \frac{1}{r} \frac{\partial}{\partial r} (r F_r) + \frac{1}{r} \frac{\partial F_\phi}{\partial \phi}$ with $\vec{F} = F_r \vec{u}_r + F_\phi \vec{u}_\phi$. In our case $F_r = \rho \dot{r}$ and $F_\phi = \rho r \dot{\phi}$. We integrate Eq. (S10) over r :

$$\varepsilon \frac{\partial f_1}{\partial \tau} + \int_0^\infty dr \left\{ (1 + \varepsilon f_1) \partial_r [\dot{r} \delta(r - 1 - \varepsilon r_1)] + \delta(r - 1 - \varepsilon r_1) \partial_\phi [\dot{\phi} (1 + \varepsilon f_1)] \right\} = 0. \quad (\text{S11})$$

Now, we replace $\frac{\partial f_1}{\partial \tau}$ by λf_1 and keep only the order ϵ terms:

$$\lambda f_1 + \tilde{\omega} \frac{\partial f_1}{\partial \phi} - 2c_2 \frac{\partial r_1}{\partial \phi} + \kappa B_0 \frac{\partial}{\partial \phi} [c_1 \cos(\Upsilon - \phi) + \sin(\Upsilon - \phi)] = 0 \quad (\text{S12})$$

and using r_1 from Eq. (S9):

$$\tilde{\omega} \partial_\phi f_1 = -\lambda f_1 + \kappa B_0 [(1 - 2c_2 B) \cos(\Upsilon - \phi) + (2c_2 A - c_1) \sin(\Upsilon - \phi)].$$

If $f_1(\phi|\tilde{\omega}) = \kappa B_0 [\mathcal{C} \cos(\Upsilon - \phi) + \mathcal{D} \sin(\Upsilon - \phi)]$:

$$\tilde{\omega} \mathcal{C} + \lambda \mathcal{D} = 2c_2 \mathcal{A} - c_1, \quad (\text{S13})$$

$$\lambda \mathcal{C} - \tilde{\omega} \mathcal{D} = 1 - 2c_2 \mathcal{B}. \quad (\text{S14})$$

The solutions are:

$$\mathcal{C} = \frac{(1 + c_1 c_2) \lambda + \tilde{\omega} (c_2 - c_1)}{\lambda^2 + \tilde{\omega}^2} - \frac{c_2 [c_1 (\lambda + 2) + \tilde{\omega}]}{(\lambda + 2)^2 + \tilde{\omega}^2}; \quad \mathcal{D} = -\frac{(1 + c_1 c_2) \tilde{\omega} + (c_1 - c_2) \lambda}{\lambda^2 + \tilde{\omega}^2} - \frac{c_2 (\lambda + 2 - c_1 \tilde{\omega})}{[\lambda + 2(1 - \epsilon)]^2 + \tilde{\omega}^2}.$$

Self-consistency condition

Our solutions for f_1 and r_1 must be consistent with Eq. (S6) (self-consistency condition). This implies:

$$2\pi = \int_{-\infty}^{\infty} d\tilde{\omega} g(\tilde{\omega}) \int_0^{2\pi} d\phi e^{i(\phi - \Upsilon)} (r_1 + f_1) / B_0 = \kappa \int_{-\infty}^{\infty} d\tilde{\omega} g(\tilde{\omega}) \int_0^{2\pi} d\phi e^{i(\phi - \Upsilon)} [(A + \mathcal{C}) \cos(\Upsilon - \phi) + (\mathcal{B} + \mathcal{D}) \sin(\Upsilon - \phi)].$$

This yields two equations for the imaginary and real parts, respectively:

$$\int_{-\infty}^{\infty} d\tilde{\omega} g(\tilde{\omega}) (\mathcal{B} + \mathcal{D}) = 0, \quad (\text{S15})$$

$$\kappa \int_{-\infty}^{\infty} d\tilde{\omega} g(\tilde{\omega}) (\mathcal{A} + \mathcal{C}) = 2. \quad (\text{S16})$$

Final result

For the stability threshold, we make $\lambda \rightarrow 0$:

$$\mathcal{A}(\lambda \rightarrow 0) = \frac{2 - c_1 \tilde{\omega}}{\tilde{\omega}^2 + 4}, \quad (\text{S17})$$

$$\mathcal{B}(\lambda \rightarrow 0) = -\frac{2c_1 + \tilde{\omega}}{\tilde{\omega}^2 + 4}, \quad (\text{S18})$$

$$\mathcal{C}(\lambda \rightarrow 0) = \pi(1 + c_1 c_2) \delta(\tilde{\omega}) + \frac{(c_2 - c_1) \tilde{\omega}}{\tilde{\omega}^2 + \lambda^2} - \frac{c_2 (2c_1 + \tilde{\omega})}{\tilde{\omega}^2 + 4}, \quad (\text{S19})$$

$$\mathcal{D}(\lambda \rightarrow 0) = \pi(c_2 - c_1) \delta(\tilde{\omega}) - \frac{(1 + c_1 c_2) \tilde{\omega}}{\tilde{\omega}^2 + \lambda^2} + \frac{c_1 c_2 \tilde{\omega} - 2c_2}{\tilde{\omega}^2 + 4}. \quad (\text{S20})$$

To obtain the boundary of incoherence we need the κ_c - and Ω_c -dependent integrals:

$$I_1 = \int d\tilde{\omega} \frac{g(\tilde{\omega})}{\tilde{\omega}^2 + 4}; \quad I_2 = \lim_{\lambda \rightarrow 0} \int d\tilde{\omega} \frac{g(\tilde{\omega}) w}{\tilde{\omega}^2 + \lambda^2} = p.v. \int g(\tilde{\omega}) \frac{d\tilde{\omega}}{\tilde{\omega}} d\tilde{\omega}; \quad I_3 = \int d\tilde{\omega} \frac{g(\tilde{\omega}) w}{\tilde{\omega}^2 + 4}; \quad I_4 = \int d\tilde{\omega} g(\tilde{\omega}) \delta(\tilde{\omega}) = g(0) \quad (\text{S21})$$

We have then:

$$-2(c_1 + c_2) I_1 - (1 + c_1 c_2) I_2 - (1 - c_1 c_2) I_3 + \pi(c_2 - c_1) I_4 = 0 \quad (\text{S22})$$

$$2(1 - c_1 c_2) I_1 + (c_2 - c_1) I_2 - (c_1 + c_2) I_3 + \pi(1 + c_1 c_2) I_4 = 2/\kappa_c \quad (\text{S23})$$

This equation determine the boundary of the UIS and the frequency of the instability Ω_c . The most efficient way to compute the stability boundary is to fix κ_c and Ω_c , compute I_i and use (S22) and (S23) to obtain c_1 and c_2 . Finally, one refers to Eq. (S1) to obtain ϵ_c .

III. DERIVATION OF EQ. (2)

In this section we apply second order phase reduction to the ensemble of globally coupled Stuart-Landau oscillators, Eq. (1). Neglecting terms of order $O(\epsilon^3)$ and $O(\epsilon^2\sigma)$ we obtain Eq. (2) in the main text.

The first step in phase reduction is performing a change of variable in Eq. (1) to phase and amplitude, $A_j = r_j e^{i(\theta_j + c_2 \ln r_j)}$. Additionally, we go to a rotating reference frame such that the frequency of the oscillator is $\sigma\omega_j$:

$$\dot{r}_j = r_j(1 - \epsilon - r_j^2) + \frac{\epsilon\Gamma}{N} \sum_{k=1}^N r_k \left\{ \sin[\theta_k - \theta_j + \gamma + c_2(\ln r_k - \ln r_j)] \right\} \quad (\text{S24a})$$

$$\dot{\theta}_j = \sigma\omega_j + \frac{\epsilon\eta}{Nr_j} \sum_{k=1}^N r_k \left\{ \sin[\theta_k - \theta_j + \alpha + c_2(\ln r_k - \ln r_j)] \right\}, \quad (\text{S24b})$$

where, for simplicity, we have defined $\Gamma = \sqrt{1 + c_1^2}$, $\tan \gamma = -1/c_1$, and η and α as in the main text.

Assuming the smallness of the coupling parameter ϵ we can expand the radial variable in this parameter $r_j = 1 + \epsilon r_j^{(1)} + \epsilon^2 r_j^{(2)} + \dots$ where the zeroth order is 1 since the limit cycle has $r = 1$. To obtain the second-order phase reduction we expand the equation (S24b) up to order ϵ^2 :

$$\dot{\theta}_j = \sigma\omega_j + \frac{\epsilon\eta}{N} \sum_{k=1}^N \sin(\theta_k - \theta_j + \alpha) + \epsilon^2 \eta \sqrt{1 + c_2^2} \left[\frac{1}{N} \sum_{k=1}^N r_k^{(1)} \sin(\theta_k - \theta_j + \alpha + \delta) - \frac{1}{N} r_j^{(1)} \sum_{k=1}^N \sin(\theta_k - \theta_j + \alpha + \delta) \right] + O(\epsilon^3) \quad (\text{S25})$$

or

$$\dot{\theta}_j = \sigma\omega_j + \epsilon\eta R \sin(\Psi - \theta_j + \alpha) + \epsilon^2 \eta \sqrt{1 + c_2^2} \left[\frac{1}{N} \sum_{k=1}^N r_k^{(1)} \sin(\theta_k - \theta_j + \alpha + \delta) - r_j^{(1)} R \sin(\Psi - \theta_j + \alpha + \delta) \right] + O(\epsilon^3) \quad (\text{S26})$$

where $\tan \delta = c_2$. Now, to close this equation we only need the radial correction up the order ϵ , i.e. $r_j^{(1)}$.

In order to obtain $r_j^{(1)}$ we assume the radii depend on the phases, $r_j = r_j(\theta)$, and apply the chain rule to (S24a), $\dot{r}_j = \sum_k \dot{\theta}_k \partial_{\theta_k} r_j$. Expanding r_j in powers of ϵ , we obtain the equation for $r_j^{(1)}$:

$$\sum_{k=1}^N \sigma\omega_k \partial_{\theta_k} r_j^{(1)} = -2r_j^{(1)} + \frac{\Gamma}{N} \sum_{k=1}^N \sin(\theta_k - \theta_j + \gamma), \quad (\text{S27})$$

whose solution is

$$r_j^{(1)} = \frac{\Gamma}{N} \sum_{k=1}^N \frac{1}{2 + \sigma^2 \frac{(\omega_k - \omega_j)^2}{2}} \sin(\theta_k - \theta_j + \gamma) - \sigma \frac{\omega_k - \omega_j}{4 + \sigma^2 (\omega_k - \omega_j)^2} \cos(\theta_k - \theta_j + \gamma). \quad (\text{S28})$$

Neglecting terms of order σ :

$$r_j^{(1)} \simeq \frac{\Gamma}{2} R \sin(\Psi - \theta_j + \gamma) \quad (\text{S29})$$

Replacing (S29) into the (S26) and using the relations $\alpha + \delta + \gamma = \beta - \pi/2$ and $-\alpha - \delta + \gamma = -\pi/2$ we obtain Eq. (2) in the main text. Notice that preserving the $O(\sigma)$ term of (S28) translates into an $O(\epsilon^2\sigma)$ term in Eq. (S26). This term is safely neglected provided that $\sigma \ll 1$. The relative importance of terms $O(\epsilon^2\sigma)$ and $O(\epsilon^3)$ depends on the ratio ϵ/σ . In conclusion, Eq. (2) in the main text is the phase reduction of Eq. (1) after neglecting terms $O(\epsilon^3)$ and $O(\epsilon^2\sigma)$.

IV. BOUNDARY OF INCOHERENCE FOR EQ. (2)

This section is devoted to deriving the boundary of the uniform incoherent state (UIS) in the enlarged Kuramoto model, Eq. (2) in the main text. In order to compute this boundary we first note that in the neighborhood of UIS ($R = Q = 0$) nonlinear terms in R and Q are negligible. Removing these nonlinear terms in the enlarged Kuramoto model, Eq. (2) in the main text, we get the classical Kuramoto-Sakaguchi model:

$$\dot{\theta}_j = \epsilon \eta R \sin(\psi - \theta_j + \alpha) + \frac{\epsilon^2 \eta^2}{4} R \sin(\psi - \theta_j + \beta) = \epsilon \hat{\eta} R \sin(\psi - \theta_j - \hat{\alpha}), \quad (\text{S30})$$

where

$$\hat{\eta} = \eta \sqrt{1 + \frac{\epsilon}{2}(1 - c_1 c_2) + \frac{\epsilon^2}{4} \eta^2}, \quad (\text{S31})$$

$$\hat{\alpha} = \arg \left\{ 1 + c_1 c_2 + \frac{\epsilon}{4}(1 + c_2^2)(1 - c_1^2) + i \left[c_1 - c_2 + \frac{\epsilon c_1}{2}(1 + c_2^2) \right] \right\}. \quad (\text{S32})$$

The transition point between UIS and partial synchrony, for a symmetric frequency distribution, satisfies [3]:

$$\epsilon_c \hat{\eta} = \frac{2 \cos \hat{\alpha}}{\pi g(\Omega_c)}, \quad (\text{S33a})$$

$$PV(\Omega_c) = \frac{\pi g(\Omega_c) \tan \hat{\alpha}}{2}, \quad (\text{S33b})$$

where Ω_c is the critical frequency at the onset of partial synchronization, which remains to be determined. The function $PV(\Omega)$ in (S33b) is defined as

$$PV(\Omega) = \lim_{a \rightarrow 0} \left(\int_{-\infty}^{-\Omega-a} + \int_{-\Omega+a}^{\infty} \right) \frac{g(\omega)}{2(\omega - \Omega)} d\omega = p.v. \int_{-\infty}^{\infty} \left[\frac{g(\omega)}{2(\omega - \Omega)} \right] d\omega. \quad (\text{S34})$$

We can now express (S33) in terms of c_1 , c_2 and ϵ_c

$$\frac{\pi g(\Omega_c)}{2} = \frac{1 + c_1 c_2 + \frac{\epsilon_c}{4}(1 + c_2^2)(1 - c_1^2)}{\epsilon_c \left\{ (1 + c_1^2)(1 + c_2^2) \left[1 + \frac{\epsilon_c}{2}(1 - c_1 c_2) + \frac{\epsilon_c^2}{4} \eta^2 \right] \right\}}, \quad (\text{S35a})$$

$$\frac{2PV(\Omega_c)}{\pi g(\Omega_c)} = \frac{c_1 - c_2 + \frac{\epsilon_c c_1}{2}(1 + c_2^2)}{1 + c_1 c_2 + \frac{\epsilon_c}{4}(1 + c_2^2)(1 - c_1^2)}. \quad (\text{S35b})$$

From these equations, we numerically compute the UIS boundary in Fig. 2(c).

-
- [1] O. V. Popovych, Y. L. Maistrenko, and P. A. Tass, "Phase chaos in coupled oscillators," *Phys. Rev. E* **71**, 065201(R) (2005).
 [2] M. C. Cross, J. L. Rogers, R. Lifshitz, and A. Zumdieck, "Synchronization by reactive coupling and nonlinear frequency pulling," *Phys. Rev. E* **73**, 036205 (2006).
 [3] H. Sakaguchi and Y. Kuramoto, "A soluble active rotator model showing phase transitions via mutual entrainment," *Prog. Theor. Phys.* **76**, 576–581 (1986).